Controlling Particle Morphology during Growth of Bayerite in Aluminate Solutions

Grégory Lefèvre,* Vincent Pichot, and Michel Fédoroff

Centre d'Etudes de Chimie Métallurgique, Centre National de la Recherche Scientifique UPR 2801, 15, Rue Georges Urbain, 94407 Vitry-sur-Seine, France

Received January 8, 2003. Revised Manuscript Received March 10, 2003

To study the influence of the orientations of the faces of metal oxyhydroxides on their surface reactivity, the synthesis of bayerite [β-$Al(OH)_3$] particles with different morphologies was studied. The growth of bayerite was performed in aqueous solution at 70 °C by continuously injecting a sodium aluminate solution and stabilizing the pH at a constant value by monitoring the injection of a nitric acid solution. The effects of the following parameters were studied: pH, flow rate of aluminate solution, total duration of synthesis, and seeding. The solids were characterized by high-resolution SEM, XRD, IR spectroscopy, thermogravimetric analysis, and surface area measurements. By choosing the growth parameters, we were able to control the morphology of particles with shapes ranging from agglomerates of rods or cones to ovoid crystallites. In certain cases, traces of gibbsite, norstandite, and pseudoboehmite were obtained in addition to bayerite, but their quantity can be minimized.

Introduction

The surface reactivity and sorption properties of solids play a major role in the migration of toxic and radioactive species in surface and underground waters in contact with solid matter. Predicting the migration of such species in natural media or in artificial barriers requires detailed knowledge of sorption data together with quantitative modeling.

The first studies on the reactivity of oxide surfaces in water used a model (called the 2-pK model) based on a single type of hydroxyl group, whose concentration is defined by a mean surface density (usually 2−10 sites·nm^{-2}).[1] Further studies showed that the use of multisite models, based on a certain number of different types of hydroxyl groups, can improve the modeling of crystallized oxides.[2,3] In these models, the characteristics (acido-basic constants, site density, etc.) of each type of hydroxyl group is related to the coordination number of surface oxygen atoms. Because this coordination number depends on the orientation of crystal faces, the surface reactivity of a solid particle should be the sum of the contributions of each exposed face. The validation of such models requires substrates with a definite proportion of faces with known orientations. The present work is focused on the synthesis of bayerite, a polymorph of hydrated alumina.

Supersaturated aluminate solutions are relaxed by precipitation of aluminum trihydroxides. In the Bayer process, gibbsite [α-$Al(OH)_3$] is the main product obtained under industrial conditions [6 M NaOH, 4.4 M $Al(OH)_3$ at 70 °C]. More dilute solutions can lead to bayerite [β-$Al(OH)_3$], whose Al−O−Al basic layer structure is identical to that of gibbsite, but with a different ordering: ABBA-type lattice for gibbsite and ABAB for bayerite. The mechanisms involved in the transformation of tetrahedral aluminate ions into octahedrally coordinated $Al(OH)_3$ crystals are as yet unknown, whereas agreement has been achieved on the existence of polymeric precursors with the formula $Al_x(OH)_y^{(y-3x)-}$.[4−6]

The diversity of crystal shapes (cones, wedges, rods, hourglass figures[7]) typical of bayerite crystallites is what led us to choose this solid as a model for studying the relationship between the morphology of the particles and their surface reactivity. Other uses of this compound are its role as a precursor in the synthesis of transition aluminas (η- and ρ-Al_2O_3),[8] as a support for metal catalysts, and as a reactant in the synthesis of Li−Al layered double hydroxide ($[LiAl_2(OH)_6]Cl{\cdot}xH_2O$), an anion exchanger.[9] Bayerite is the $Al(OH)_3$ polymorph usually found on aluminum corroded in hot water[7] or in cold water after amalgamation.[10] It is obtained by the aging of alumina gels[11,12] and transition aluminas[8,13,14] in water. The acidification of an aluminate solution with $HClO_4$,[15] HNO_3,[3,5] or CO_2[16] leads to bayerite with some

* To whom correspondence should be addressed. Telephone: 33 1 56 70 30 54. Fax: 33 1 46 75 04 33. E-mail: lefevre@glvt-cnrs.fr.

(1) Dzombak, D. A.; Morel, F. *Surface Complexation Modeling. Hydrous Ferric Oxide*; John Wiley & Sons: New York, 1990.
(2) Hiemstra, T.; Van Riemsdijk W. H.; Bolt, G. H. *J. Colloid Interface Sci.* **1989**, *133*, 91.
(3) Hiemstra, T.; Yong, H.; Van Riemsdijk, W. H. *Langmuir* **1999**, *15*, 5942.
(4) Gerson, A. R.; Ralston, J.; Smart R. S. C. *Colloid Surf. A* **1996**, *110*, 105.
(5) Van Straten, H. A.; Schoonen, M. A. A.; De Bruyn, P. L. *J. Colloid Interface Sci.* **1985**, *103*, 493. Van Straten, H. A.; Holtkamp, B. T. W.; De Bruyn, P. L. *J. Colloid Interface Sci.* **1984**, *98*, 342. Van Straten, H. A.; De Bruyn, P. L. *J. Colloid Interface Sci.* **1984**, *102*, 260.
(6) Renaudin, G.; François, M. *Synth. React. Inorg. Met.−Org. Chem.* **1997**, *27*, 947.
(7) Alwitt, R. S. In *Oxides and Oxide Films*; Diggle, J. W., Vijh, A. K., Eds.; Marcel Dekker: New York, 1976; Vol. 4, p 169.
(8) Tertian, R.; Papée, D. *J. Chim. Phys.* **1958**, *55*, 341.
(9) Fogg, A. M.; Freij A. J.; Parkinson, G. M. *Chem. Mater.* **2002**, *14*, 232.
(10) Schmäh, H. *Z. Naturforsch.* **1946**, *1*, 323.
(11) Music, S.; Dragcevic, D.; Popovic, S.; Vdovic, N. *Mater. Chem. Phys.* **1999**, *59*, 12.
(12) Souza-Santos, P.; Vallejo-Freire, A.; Souza-Santos, H. L. *Kolloid Z.* **1953**, *133*, 101.

10.1021/cm0310059 CCC: $25.00
Published on Web 05/17/2003

impurities in the form of gibbsite and pseudoboehmite. In these studies, the acid was slowly added to the aluminate solution, so that the pH and the dissolved aluminum concentration decreased throughout the duration of the experiment. We have developed a method designed to control the growth of bayerite crystals that is based on the neutralization of an aluminate solution by its slow addition into a reactor whose pH is monitored and kept constant by the addition of a HNO_3 solution.[17] The first results obtained with this method (detailed in ref 17) illustrated its ability to synthesize bayerite micro-rods, whereas the usual titration method with varying pH gives rise to a diversity of shapes.

In the present work, we have performed a systematic investigation of the influence of several synthesis parameters on the purity and morphology of bayerite. The studied parameters were pH, flow rate and amount of aluminate addition, and seeding. As in previous works, X-ray diffraction, nitrogen adsorption, and scanning electron microscopy were used to determine the different morphologies obtained. These methods were complemented by infrared spectroscopy and thermogravimetric analysis, together with thermodynamic and kinetic calculations.

Experimental Section

Synthesis. Bayerite was synthesized by a method originally designed for apatite growth[18] and layered double hydroxide synthesis,[19] modified to study aluminum hydroxide crystallization.[17] This experimental setup allows the synthesis to be carried out at a constant pH (from 9.4 to 10.8) throughout the aluminum hydroxide precipitation. The synthesis is conducted as follows: Initially, 300 mL of a solution of NaOH, whose concentration was adjusted to achieve the pH value of the experiment (a value of 12.8 was used for the dissociation constant pK_w of water at 70 °C[20]), was heated in a closed PMP 1-L vessel at 70 ± 1 °C by a water bath, with moist argon gas over the solution. This temperature was chosen to minimize the precipitation of amorphous phases or other phases such as pseudoboehmite.[5] A 0.1 M sodium aluminate solution with a known concentration of sodium hydroxyde was added at a constant flow rate (from 28 to 46 mL/h) by a peristaltic pump. The actual flow rate was measured before and after each experiment. The pH was measured by a combined glass electrode (Mettler Toledo) connected to a pH meter (Metrohm 691). The pH calibration was done at 70 °C with two buffers. The first was a commercial standard (Mettler Toledo) whose pH dependence on temperature is small (from 7.00 at 25 °C to 6.97 at 50 °C). Because the pH of alkaline buffers strongly depends on temperature, we prepared a sodium tetraborate decahydrate solution (3.81 g/L), which has a pH value of 8.92 at 70 °C.[20] The pH was kept constant, under monitoring by a computer and homemade software, by injecting increments of 0.5 mL of 0.2 M HNO_3 with an automatic titrator (Metrohm). In some experiments, seeds of bayerite prepared during a preceding synthesis were put into the solution before the aluminate solution was introduced. The experimental conditions of the prepared samples are listed in Table 1. Synthesized samples are denoted as follows: U or S for an unseeded or seeded experiment, pH (×10), plus characteristics of the synthesis, if relevant (Sh, short; Lo, long; Ra, rapid; Sl, slow; W, weakly seeded; H, highly seeded; or D, initial dissolved aluminate). Thus, U98Ra is the sample synthesized in an unseeded experiment conducted at a pH of 9.8 with rapid addition of aluminate.

Table 1. Experimental Conditions for the Preparation of Bayerite Samples[a]

sample	synthesis pH	aluminate solution flow rate (mL/h)	total volume of aluminate (mL)	initial solution characteristics
U94	**9.4**	28.5	97	NaOH, pH 9.4
U96	**9.6**	29.5	92	NaOH, pH 9.6
U98	**9.8**	27.7	98	NaOH, pH 9.8
U102	**10.2**	29.1	86	NaOH, pH 10.2
U104	**10.4**	28.9	98	NaOH, pH 10.4
U108	**10.8**	33.7	109	NaOH, pH 10.8
U98Sh	9.8	33.6	**57**	NaOH, pH 9.8
U98Lo	9.8	32.9	**230**	NaOH, pH 9.8
U98Ra	9.8	**45.6**	93	NaOH, pH 9.8
U98Sl	9.8	**21.1**	95	NaOH, pH 9.8
S100W	10.0	36.0	97	NaOH, pH 10.0, **50 mg of bayerite**
S100H	10.0	34.5	95	NaOH, pH 10.0, **200 mg of bayerite**
S100D	10.0	33.2	101	NaOH, pH 10.0, **2.1 mM aluminate**

[a] Studied parameters are in bold face, initial volume of solution is 300 mL.

Once the aluminate solution was entirely poured into the reaction vessel, the pH was brought to about 8 by the addition of nitric acid. The precipitate was left in the mother liquid overnight at room temperature. It was then filtered on 0.2-μm porosity membranes and washed with deionized water (16 MΩ·cm). After drying in a desiccator in the presence of silica gel, about 500 mg of a fine white powder was obtained in each experiment.

Characterization of Solids. X-ray diffractograms (XRDs) were recorded using a Co Kα radiation. Surface areas were determined by nitrogen adsorption and desorption, performed with a Coulter SA3100 area analyzer, after degassing of the samples for 30 min at 120 °C. High-resolution scanning electron microscopy (SEM) was performed using a Leo DSM 982 Gemini instrument, the powders being deposited on a carbon ribbon and metallized with Pt/Pd. Infrared spectroscopy was carried out on a paste made by a mixture of the powder with Fluorolube placed between two CaF_2 windows with a Perkin-Elmer 1720 spectrometer monitored by Spectrum V2.00 software. Thermogravimetric measurements were carried out by heating the sample in a ceramic crucible at 200 °C for 1 h and then at 1200 °C for 1 h. The sample was then cooled in a desiccator and weighed.

Results and Discussion

Growth Rate of the Solid Phase. The volume of acid added to maintain a constant pH was recorded as a function of time. An example of such data recorded at pH 9.8 is showed in Figure 1a.

In the pH range (9.4−10) used in these experiments, $Al(OH)_4^-$ is the only soluble species of aluminum.[21] Protons are involved in two reactions

$$H^+ + OH^- \rightarrow H_2O \quad (1)$$

$$H^+ + Al(OH)_4^- \rightarrow Al(OH)_3\downarrow + H_2O \quad (2)$$

(13) Lefèvre, G.; Duc, M.; Lepeut, P.; Caplain R.; Fédoroff, M. *Langmuir* **2002**, *18*, 7530.
(14) Chen, Y.; Hyldtoft, J.; Jacobsen, C. J. H.; Nielsen O. F. *Spectrochim. Acta A* **1995**, *51*, 2161.
(15) Schoen, R.; Roberson, E. *Am. Mineral.* **1970**, *55*, 43.
(16) Phambu, N. Ph.D. Thesis, University of Nancy I, Nancy, France, 1996
(17) Lefèvre, G.; Fédoroff, M. *Mater. Lett.* **2002**, *56*, 978.
(18) Jeanjean, J.; McGrellis, S.; Rouchaud, J. C.; Fédoroff, M.; Rondeau, A.; Perocheau, S.; Dubis, A. *J. Solid State Chem.* **1996**, *126*, 195.
(19) Prinetto, F.; Ghiotti, G.; Graffin, P.; Tichit, D. *Microporous Mesoporous Mater.* **2000**, *39*, 229
(20) Galster, H. *pH Measurement—Fundamentals, Methods, Applications, Instrumentation*; VCH Verlag: Weinheim, Germany, 1991.
(21) Wefers, K.; Misra, C. *Oxides and Hydroxides of Aluminium*; Alcoa Technical Paper No. 19, Alcoa: Pittsburgh, PA, 1987.

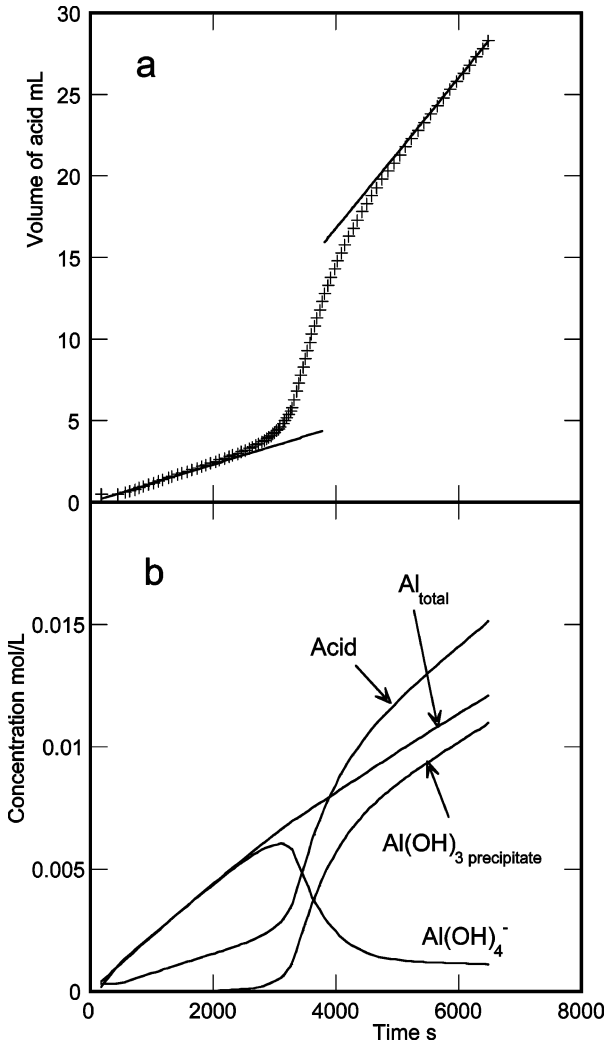

Figure 1. Typical data obtained from a synthesis experiment. (a) Volume of nitric acid solution added to keep a constant pH versus time, with fitting before precipitation and when an equilibrium of precipitation is achieved. (b) Variation of the concentrations of nitric acid, total aluminum, free aluminate, and aluminum precipitated as trihydroxide.

The variation of the quantity of added nitric acid shows two linear sections separated by a curved one. The first part corresponds to reaction 1 alone: aluminum hydroxide does not precipitate, and the solution becomes supersaturated with respect to aluminate ions.

The electrical neutrality of the solution, neglecting H^+ ions in this pH range, can be represented as

$$[Na^+] = [NO_3^-] + [OH^-] + [Al(OH)_4^-] \quad (3)$$

The different terms of this equation can be calculated as follows

$$[Na^+] = \frac{k_{Na}C_{Al}rt}{V_0 + v_{ac} + rt} + \frac{K_w V_0}{a_{H^+}\gamma_{OH}(V_0 + v_{ac} + rt)} \quad (4)$$

where the last term represents the concentration of Na^+ resulting from the adjustment of the pH of this initial solution by the addition of NaOH

$$[NO_3^-] = \frac{C_{ac}v_{ac}}{V_0 + v_{ac} + rt} \quad (5)$$

$$[OH^-] = \frac{K_w}{a_{H^+}\gamma_{OH}} \quad (6)$$

$$[Al(OH)_4^-] = \frac{(1 - f)C_{Al}rt}{V_0 + v_{ac} + rt} \quad (7)$$

where k_{Na} is the sodium-to-aluminum ratio in the added aluminate solution; C_{Al} is the concentration of aluminum in this solution; r is the flow rate of this solution; t is the time; V_0 is the initial volume; v_{ac} is the volume of nitric acid added; C_{ac} is the concentration of the nitric acid solution; K_w is the ionization constant of water; a_{H^+} is the activity of H_3O^+ ions as deduced from pH measurements; γ_{OH} is the activity coefficient of OH^- ions (calculated by the Debye−Hückel equation), which is used here because pH measurements lead to activities and not to concentrations as are used in eq 3; and f is the fraction of aluminum precipitated ($f = [Al]_{prec}/[Al]_{total}$).

From eqs 3−7, the variation of the added acid volume, v_{ac}, can be calculated as a function of time t as

$$v_{ac} = \frac{\left[(k_{Na} - 1 + f)C_{Al} - \frac{K_w}{a_{H^+}\gamma_{OH}}\right]rt}{C_{ac} + \frac{K_w}{a_{H^+}\gamma_{OH}}} \quad (8)$$

When precipitation does not occur ($f = 0$), eq 8 becomes

$$v_{ac} = \frac{\left[(k_{Na} - 1)C_{Al} - \frac{K_w}{a_{H^+}\gamma_{OH}}\right]rt}{C_{ac} + \frac{K_w}{a_{H^+}\gamma_{OH}}} \approx \frac{(k_{Na} - 1)C_{Al}rt}{C_{ac}} = p_1 t \quad (9)$$

where p_1 can be identified as the slope of the first linear part of the curve in Figure 1a.

When the aluminum hydroxide precipitate is in equilibrium with the solution, the activity of the $Al(OH)_4^-$ ions is constant and can be calculated from the solubility product of $Al(OH)_3$

$$K_{so} = \frac{a_{Al^{3+}}}{(a_{H^+})^3} \quad (10)$$

K_{so} is related to the constant $K_{S4} = a_{OH^-}/a_{Al(OH)^{4-}}$ of the reaction

$$Al(OH)_4^- \rightleftharpoons \beta\text{-}Al(OH)_3 + OH^- \quad (11)$$

by the expression

$$K_{S4} = \frac{K_w}{K_{so}{}^*\beta_4} \quad (12)$$

where $^*\beta_4$ is the fourth hydrolysis constant of Al^{3+} ions.

In this case

$$v_{ac} \approx \frac{k_{Na} C_{Al} r t}{C_{ac}} - \frac{[Al(OH)_4^-]V}{C_{ac}}$$
$$\approx p_2 t - a \quad (13)$$

where V is the total volume of the solution, a represents an almost constant value, and p_2 can be indentified as the slope of the second linear part of the curve in Figure 1a.

From the general formula for v_{ac} (eq 8), it is also possible to calculate the quantities and the concentrations of total, dissolved, and precipitated aluminum in the solution during the precipitation process. The variations of these concentrations are shown in Figure 1b. As expected, the concentration of $Al(OH)_4^-$ reaches a constant value, from which it is possible to calculate the solubility constant K_{S4}. From experiments in a pH range of 9.6−10.4, using the Debye−Hückel formula for the calculation of activity coefficients, we obtain a mean value of 1.0 ± 0.1 for K_{S4}. This result is comparable to the value of 1.5 ± 0.3 measured by Verdes et al.[22] at 65 °C and pH ≈ 8.5.

During the intermediate or relaxation period, the precipitation of hydroxide leads to a decrease of the aluminate concentration in the supersaturated solution. The evolution of this concentration as a function of time can be used to determine kinetic parameters such as reaction orders. The kinetics of the growth of aluminum hydroxide was studied by Van Straten et al.[5] in the case of the titration of an aluminate solution by nitric acid. In our method, which uses a continuous flow of aluminate solution instead of a constant total aluminum concentration, the kinetic equations have to be rewritten.

The growth rate R is the derivative of the quantity of precipitated aluminum Al_{prec} as a function of time

$$R = \frac{dAl_{prec}}{dt} \quad (14)$$

In the theory of the relaxation of supersaturated solutions,[5] the growth rate is supposed to be proportional to the surface area A of the precipitate and to depend on Π, the supersaturation factor, by an exponent n, that is

$$R = k_1 A \Pi^n \quad (15)$$

with $\Pi = [Al(OH)_4^-]/[Al(OH)_4^-]_{eq}$, where $[Al(OH)_4^-]_{eq}$ is the concentration of this species at the equilibrium of precipitation and k_1 is a constant.

By approximating the surface area as $A = k_2 Al_{prec}^{2/3}$, since, in spherical or cubic particles, A is proportional to the mass to the power $^2/_3$, eq 15 becomes

$$R = k_3 Al_{prec}^{2/3} \Pi^n \quad (16)$$

where k_2 and k_3 are constants.

A plot of $\ln(R/Al_{prec}^{2/3})$ as a function of $\ln(\Pi)$, if linear, allows for the calculation of the exponent n.

An example of such a plot is shown in Figure 2, and results for different pH values are listed in Table 2. The

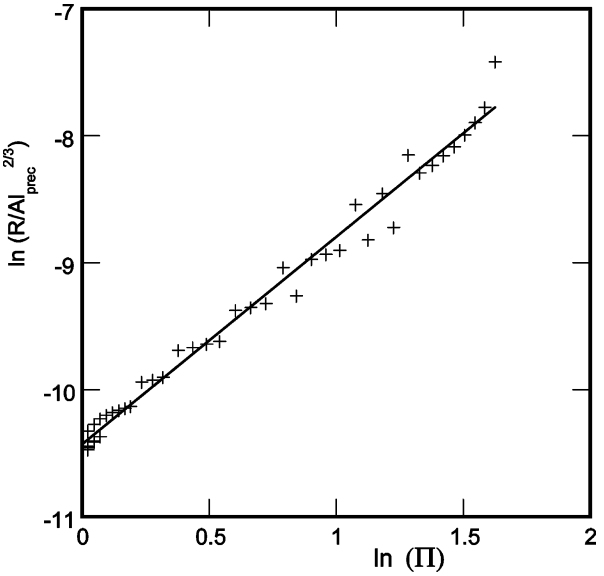

Figure 2. Example of the variation of $\ln(R/Al_{prec}^{2/3})$ versus $\ln(\Pi)$, where R is the growth rate, Al_{prec} is the quantity of aluminum precipitated, and Π is the supersaturation factor (see eqs 15 and 16).

Table 2. Synthesis Parameters for Different pH Values*

pH	t^a (min)	$[Al(OH)_4^-]^b$ (mM)	n^c
9.4	23	0.67 ± 0.06	0.98 ± 0.07
9.6	15	0.79 ± 0.01	1.06 ± 0.03
9.8	39	1.15 ± 0.01	1.38 ± 0.03
10.2	62	3.05 ± 0.02	1.61 ± 0.02
10.4	83	5.16 ± 0.02	1.92 ± 0.04
10.8	143	nd[d]	nd[d]

[a] t = precipitation time. [b] $[Al(OH)_4^-]$ = concentration of $Al(OH)_4^-$ at the end of precipitation. [c] n = exponent of the variation of R/A as a function of Π^n (eq 15 and Figure 2). [d] nd = not determined

reaction order n varies from 1 for the lowest pH to 2 for the highest pH. In titration experiments,[5] the extreme values (1 and 2) were found to be attributable to the formation of pseudoboehmite and bayerite, respectively. The fractional figures (about $^4/_3$ and $^5/_3$ found in our case for pH's 9.8 and 10.2, respectively) cannot be mathematically explained by the formation of a mixture of two hydroxides, but they would be consistent with the existence of polymeric precursors with the general formula $Al_x(OH)_y^{(y-3x)-}$.[4−6] The effect of pH might result from its influence on the nature of these polymeric species. The lack of experimental data on the stability of polymeric aluminum species does not allow us to draw further conclusions about the precipitation mechanisms. However, the variation of n indicates that the growth mechanism varies with pH, which might explain why this factor has an influence on the morphology and composition of the particles.

Effect of pH on the Composition and Morphology of the Solid Phases. Van Straten et al.[5] have observed that a slight difference in pH (0.5 unit) can change the main product of the precipitation. For the lowest pH values, amorphous compounds are obtained. As the pH increases, bayerite is formed and then gibbsite for the most alkaline solutions. Because the precipitation takes place at constant pH in our method of synthesis, we have looked for the conditions leading to bayerite, with the smallest quantity of other phases. XRD was used to detect crystalline phases, while

(22) Verdes, G.; Gout, R.; Castet, S. *Eur. J. Mineral.* **1992**, *4*, 767.

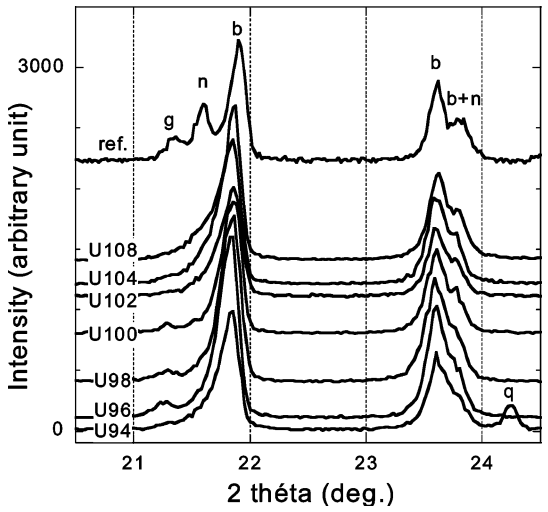

Figure 3. X-ray diffraction patterns of solids obtained for different pH values (9.4−10.8), for sample U94 mixed with quartz as an internal reference (q). Comparison with a mixture of (g) gibbsite, (n) nordstrandite, and (b) bayerite (ref).

thermogravimetric methods were used to detect amorphous compounds.

The main diffraction line of the three $Al(OH)_3$ polymorphs is located around 21.5° (2Θ), which makes the distinction between these compounds difficult. Rehydration of γ-alumina at room temperature gives a small amount of these three polymorphs, leading to a broad asymmetric peak of the mixture.[13] We have carried out rehydration experiments at 70 °C, which increases the amount of hydrated phases and allows us to distinguish the three polymorphs. A comparison between this reference and the synthetic bayerite indicates that the major compound in all samples is bayerite (Figure 3). Traces of gibbsite were detected in samples U96 and U98 according to a small line at ca. 21.2°, while the shoulder at 21.5° was attributed to the presence of traces of norstandite in samples U102 to U108, together with an increase in the relative intensity of the shoulder at 23.7°. The diffraction patterns never indicate the presence of AlOOH phases (boehmite or diaspore).

These results indicate that the synthesis between pH 9.4 and 10.8 leads to minute quantities of crystalline impurities, gibbsite for the lowest pH values and nordstrandite for pH values greater than 10. In previous works, to our knowledge, the presence of the latter phase was not mentioned.[5,11,23] However, it appears from our observations that this compound might not have been detected because of the location of its main diffraction line between those of gibbsite and bayerite.

The other impurity often found during the synthesis of aluminum trihydroxides is pseudoboehmite, but its amorphous character makes its detection by XRD difficult. An efficient method for quantifying it in a mixture with $Al(OH)_3$ phases is the measurement of the mass loss upon heating. The complete dehydration of both $Al(OH)_3$ and pseudoboehmite polymorphs leads to α-alumina (reactions 17 and 18, respectively)

$$Al(OH)_3 \rightarrow {}^1/_2\alpha\text{-}Al_2O_3 + {}^3/_2H_2O \qquad (17)$$

$$AlOOH \rightarrow {}^1/_2\alpha\text{-}Al_2O_3 + {}^1/_2H_2O \qquad (18)$$

From the stoichiometry of these equations, the mass loss

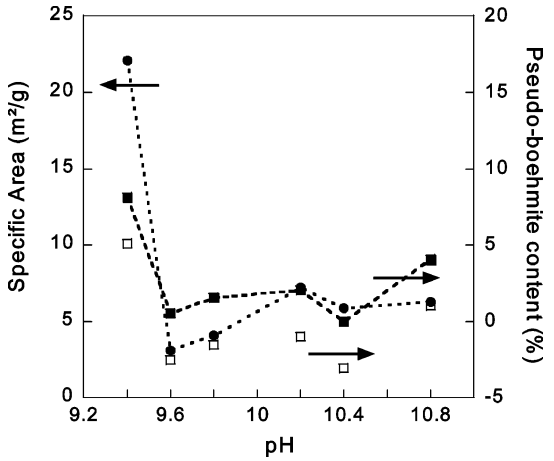

Figure 4. Comparison of specific area (●) and calculated pseudoboehmite content without correction (□) or with correction (■) for total mass loss upon heating of samples synthesized at different pH values.

obtained by the dehydration of m grams of pure compounds [Δm_{tri} and Δm_{pb} for $Al(OH)_3$ and pseudoboehmite, respectively] can be calculated as

$$\Delta m_{tri} = m/M_{tri} \times {}^3/_2 M_{H_2O} \qquad (19)$$

$$\Delta m_{pb} = m/M_{pb} \times {}^1/_2 M_{H_2O} \qquad (20)$$

where M is the molar mass. Values equal to 34.6 and 15.0% are calculated for Δm_{tri} and Δm_{pb}, respectively. For a sample with a content x_{pb} (%) of pseudoboehmite, the total relative mass loss can be defined as

$$\Delta m_{tot} = \frac{x_{pb}}{100}\Delta m_{pb} + \frac{(100 - x_{pb})}{100}\Delta m_{tri} \qquad (21)$$

which leads to the following formula for the calculation of x_{pb}

$$x_{pb} = 100\frac{\Delta m_{tot} - \Delta m_{tri}}{\Delta m_{pb} - \Delta m_{tri}} \qquad (22)$$

However, a slight error on Δm_{tot} has a large effect on the accuracy on x_{pb}. Thus, an absolute error of 0.3% in Δm_{tot} (value found in triplicate measurements) leads to an absolute error of 1.5% in x_{pb}. Another problem is the role of physisorbed water in the determination of Δm_{tot}. To remove this excess water, our procedure consists of heating the sample at 200 °C, leading to a mass loss of less than 1% for nonporous particles to more than 10% for high-specific-surface-area alumina.[13] This procedure might remove physisorbed water only partially and overestimate Δm_{tot}. The results of the analysis of our samples synthesized between pH 9.4 and 10.4 are shown in Figure 4 (open squares). It appears that several values of the pseudoboehmite content were negative. This is a consequence of the overestimation of Δm_{tot}, since the smallest value corresponds to a Δm_{tot} of 35.2%, i.e., an overestimate of 0.6%, which is assumed to be constant for similar surface areas. From this observation, we have applied a correction of 0.6% to Δm_{tot}. The

(23) Sato, T. In *Industrial Crystallization*; Jancic, S. J., De Jong, E. J., Eds.; Elsevier: New York, 1984; Vol. 84, p 391.

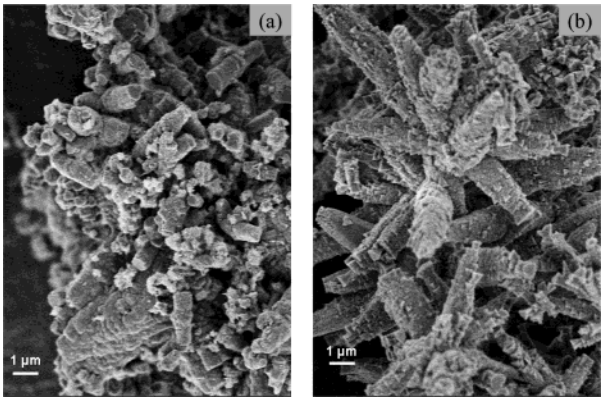

Figure 5. Scanning electron micrographs of samples synthesized at (a) pH 9.4 and (b) pH 10.4. Comparison can be made with Figure 6B (pH 9.8).

corrected pseudoboehmite contents are reported in Figure 4 (filled squares). The greatest impurity content was obtained in the sample synthesized at pH 9.4 (8%), and the other results are scattered between 0 and 4%. Moreover, these calculations were made with the ideal composition $Al_2O_3 \cdot H_2O$ for pseudoboehmite. However, this compound generally contains more water than indicated by the 1:1 H_2O/Al ratio, although no agreement has been reached in defining the location of the excess water.[21] A higher H_2O/Al ratio would increase the pseudoboehmite content calculated from the mass loss on heating.

The contents of pseudoboehmite are small, but because pseudoboehmite exhibits a high specific surface area (200−300 m^2/g)[5,8] whereas bayerite has a smaller one (a few square meters per gram), such contents have a high impact on the total specific surface area and, hence, on the surface reactivity. The measured values of surface area are consistent with the contents of pseudoboehmite (Figure 4, filled circles): a value of 22 m^2/g was found for U940 (synthesized at pH 9.4), but the other samples led to surface areas of only about 5 m^2/g. This value figure corresponds to a mean particle size of 0.5 μm, consistent with the micro-rods previously observed by SEM.[17] However, it appears that the high specific surface area obtained for samples synthesized at pH 9 can be attributed to a high pseudoboehmite content, rather than to the presence of bayerite as thin plates, as previously assumed.[17] IR spectra of samples synthesized at various pH values were recorded (not shown), and the intensity of the line observed at 3453 cm^{-1}, assigned to the stretching of surface hydroxyl groups,[13,16] was similar regardless of the pH of synthesis, in agreement with an almost constant specific surface area.

Morphologies obtained for pH 9.4, 9.8, and 10.4 (shown in Figures 5a, 6B, and 5b, respectively) indicate an effect of pH on the shape of particles. For the lowest values, short, ill-defined micro-rods are observed, mixed with pseudoboehmite "spheres", whereas only bunches of cones, revealing a common nucleus, are found for the highest pH values. Thus, the extreme values of pH lead to the growth of bayerite from numerous small nuclei, whereas at pH 9.8, the growth of micro-rods indicates a smaller number of nuclei that takes place preferentially on the bayerite rods. For the lowest pH values, the nuclei could be the pseudoboehmite phase. The highest pH values correspond to the longest induction time before precipitation, which might favor the formation of aluminum oxide polymers that act as nuclei for the bunches of cones.

Table 3. Influence of Aluminate Solution Flow Rate and Duration of Synthesis on the Specific Surface Area[a]

flow rate (mL/h)	duration (h)	sample	specific surface area (m^2/g)
27.7	3.5	U98	4.1
45.6	2	U98Ra	9.4
21.1	4.5	U98Sl	3.8
33.6	**1,7**	U98Sh	21
32.9	**7**	U98Lo	2.3

[a] Studied parameters are in bold face.

Effects of Other Synthesis Parameters. The method of synthesis used in this work allows the value of each parameter to be modified separately so that its influence on bayerite growth can be studied. We have compared characteristics of samples obtained with (1) various flow rates of the aluminate solution and (2) various durations of addition of this solution. Details are reported in Table 3.

Micrographs of samples U98Ra, U98, and U98Sl are shown in Figure 6A−C, respectively, for growth at pH 9.8. For the highest pump rate (A), two morphologies are observed: (a) agglomerates of thin rods of approximately 2 × 5 μm size and (b) micronic cone-shaped or rod-shaped crystallites. For a lower pump rate (Figure 6B), cones are still observed (a), but micro-rods constitute the most typical shape (b). For the lowest pump rate (Figure 6C), the bayerite appears only as ovoid particles.

Micrographs of samples U98Sh and U98Lo are shown in Figure 7A and B. The morphologies observed in Figure 7A are nearly the same as those found for sample U98Ra (Figure 6A). The SEM image of U98Lo reveals ovoid particles very similar to those found in U98Sl (Figure 6C). A short precipitation duration has the same final effect as rapid aluminate addition. Increasing the addition rate leads to a larger number of nuclei, but increasing the duration of the synthesis tends to increase the size of the crystallites.

On the other hand, a decrease of the pump rate or an increase of the synthesis duration leads to micro-rods, whose edges become the main nuclei for bayerite growth, leading to ovoid shapes.

Agglomerates of thin rods or cones have a higher surface area than ovoid crystallites, and the lowest area (2.3 m^2/g) was obtained for the longest experiment. However, the high specific areas measured for high pump rates and short experiments cannot be attributed to bayerite particles alone, as previously assumed,[17] as a certain amount of pseudoboehmite is present. Infrared spectra of samples with different durations of synthesis are shown in Figure 8. The line observed at 3453 cm^{-1} is assigned to surface hydroxyl groups;[13,16] thus, its relative intensity and the specific surface area are correlated. The intensity of this line decreases with increasing duration of the experiment, confirming the decrease in the surface area. The line at 3619 cm^{-1} is attributed to gibbsite,[16] and the increase of its intensity is consistent with the diffraction pattern (not shown), indicating that the amount of gibbsite is greatest for the longest synthesis.

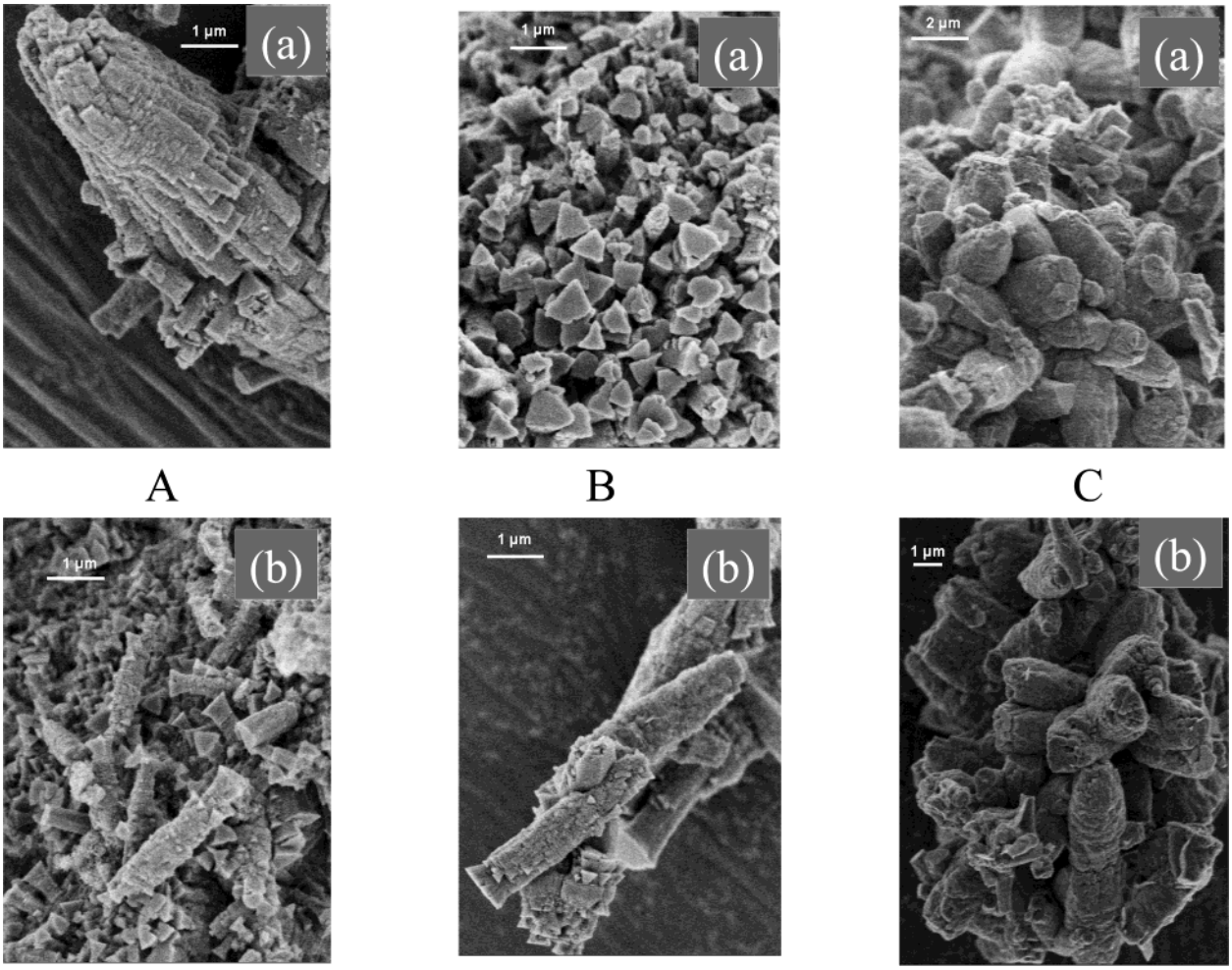

Figure 6. Scanning electron micrographs of samples synthesized at pH 9.8 with different addition rates of aluminate solution: (A) 45.6 mL/h (U98Ra), (B) 27 mL/h (U98), and (C) 21.1 mL/h (U98Sl)

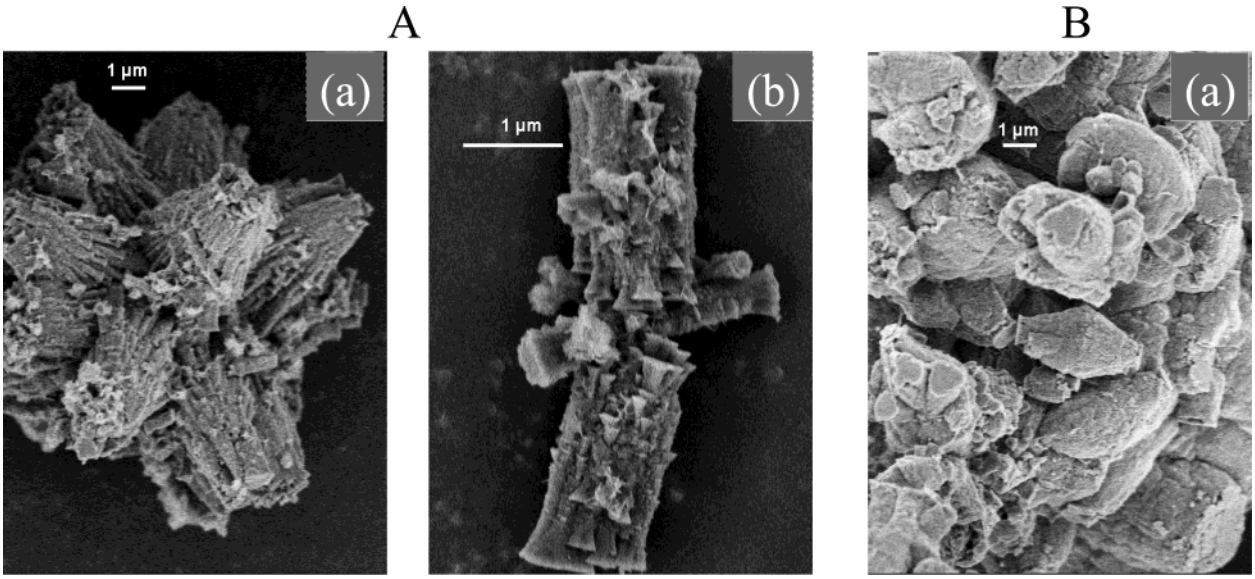

Figure 7. Scanning electron micrographs of samples synthesized at pH 9.8 with different total aluminate volumes: (A) 56 and (B) 230 mL. Comparison can be made with Figure 6B (98 mL).

Figure 9 summarizes the effects of the main parameters of synthesis on the habits of the bayerite crystals and the types of impurities present. These effects are discussed in detail in the Conclusion section.

Effect of Seeding. Because of the long induction time, the precipitation of crystalline aluminum hydroxide is performed in industrial Bayer liquors by seeding with gibbsite or bayerite crystals.[23] Several studies were published about the effect of seeding on precipitation kinetics.[23−25] The induction time can fall to an unmea-

(24) Brown, N. *J. Cryst. Growth* **1975**, *29*, 309.

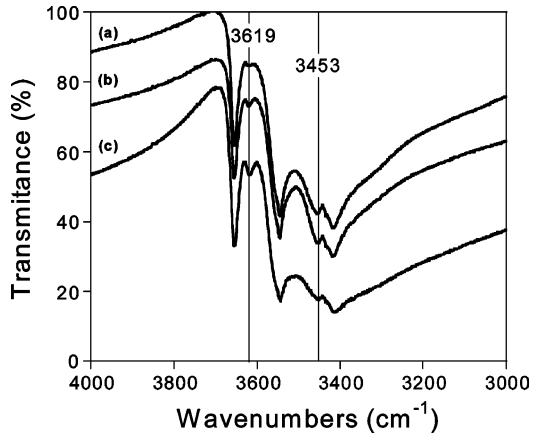

Figure 8. Infrared spectra of solids synthesized at pH 9.8 after different times of addition of aluminate solution: (a) 1 h (shifted upward by 15% for a better clarity), (b) 2.5 h, and (c) 6 h.

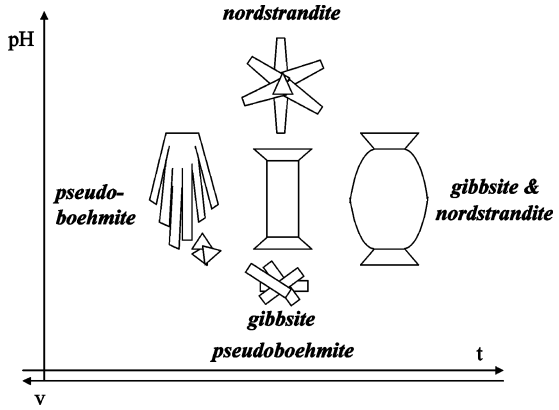

Figure 9. Habits of bayerite crystals and impurities present in relation to the parameters of the synthesis: pH, pump rate (*v*), and time of synthesis (*t*).

surable value if a large amount of seeds is used. The origin of the effect of seeding remains unclear, allowing several explanations. Precipitation can be induced by crystal growth on seed particles, leading to the formation of dendritic-like structures.[26] In a laboratory batch crystallizer equipped with a marine propeller ensuring a stirring rate of 350 rpm, Brown[24] assumed that all new hydroxide particles were removed from the seed crystal surfaces before the actual nucleation process was observed. In an unstirred reactor, Gerson et al.[25] observed that the majority of growth did not occur on the seed crystals and proposed that the effect of seeding is the partial dissolution of molecular pieces of seeds that then act as nuclei for further crystal growth.

We have carried out two experiments with different amounts of seeds of bayerite (Figure 10a,b). The supersaturation time clearly decreases and almost disappears for the higher seed amount (a). For comparison, the result of a synthesis performed without seeds but with an initial aluminate concentration of 2.1 mM is shown in Figure 10c. The supersaturation value is higher than the value reached in seed experiments, demonstrating that the effect of seeds is not partial dissolution, which

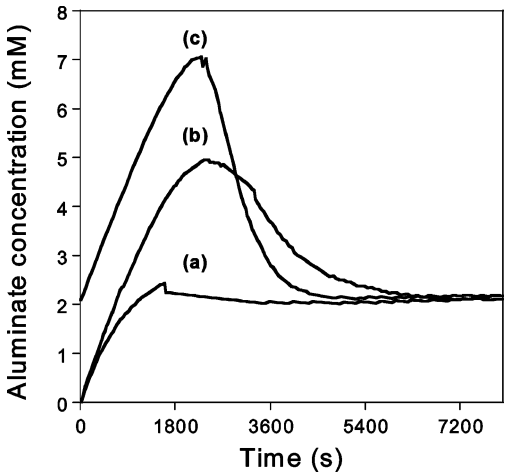

Figure 10. Relaxation curves for growth experiments seeded with (a) 200 mg of bayerite, (b) 50 mg of bayerite, and (c) with an initial aluminate concentration of 2.1 mM without seeds.

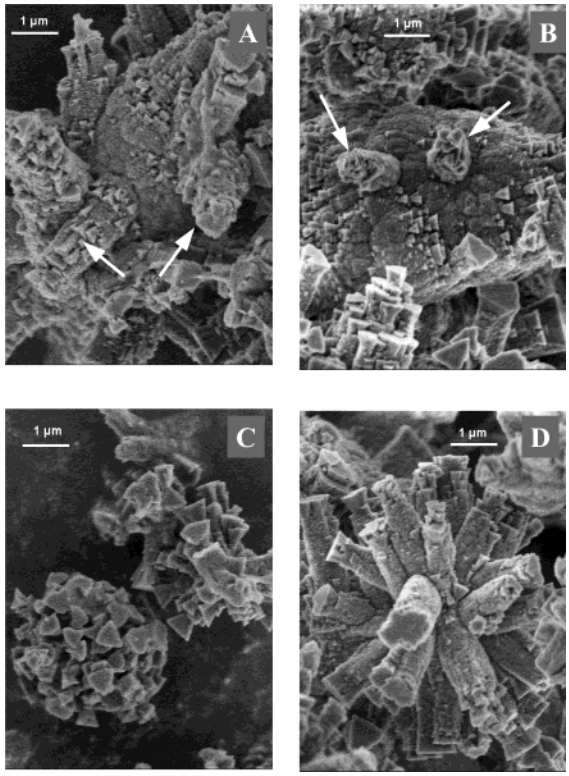

Figure 11. Scanning electron micrographs of particles of samples obtained from experiment S10-200 (seeded with 200 mg of bayerite). Dendritic structures are indicated by arrows.

would release aluminate ions. SEM images of a sample obtained from seeded synthesis (S10-200) are shown in Figure 11. Two main habits are observed: (1) dendritic growth (Figure 11A,B) and (2) bunches of small cones (Figure 11C) or rods (Figure 11D). The dendritic-like structures were observed only in the seeded experiments, and it appears that the growth of bayerite on the seeds is not epitaxial, since the growth directions of the seeds and of the newly formed bayerite are roughly perpendicular.

This result confirms that seeding of supersaturated aluminate solutions by a trihydroxide polymorph (gibbsite or bayerite) leads to the most stable solid under the conditions of the synthesis, without any influence of the crystal structure of the seed.[25] The bunch structures

(25) Gerson, A. R.; Counter J. A.; Cookson D. J. *J. Cryst. Growth* **1996**, *160*, 346.
(26) Mullin J. W. *Crystallization*, 3rd ed.; Butterworth-Heinemann: Woburn, MA, 1997.

indicate the presence of a common nucleus. However, they are also observed for unseeded syntheses at high pH values, so it is difficult to assert whether their starting points are small particles (or seeds) or polymeric precursors.

Conclusion

The use of a constant-pH method of synthesis enabled us to control the value of several parameters and to direct the growth of bayerite into several different morphologies. The effects of pH, experiment duration, and pump rate are illustrated in Figure 9, indicating that the two latter parameters have opposite effects.

Pseudoboehmite is the main impurity at low pH values or high pump rates. Because of the high specific surface area of this compound, its presence might disturb the reactivity study of bayerite synthesized under these conditions. However, this amorphous phase is thermodynamically unstable, and it might be transformed into crystallized $Al(OH)_3$ by aging of the suspension.[21] Moreover, because the dissolution rate of bayerite in acidic media is low,[13] washing the product with a dilute acid solution might selectively dissolve pseudoboehmite. Traces of gibbsite and nordstrandite are obtained for the longest syntheses, gibbsite for the lowest pH values, and nordstrandite for the highest ones. Well-defined morphologies are observed for the longest syntheses and the highest pH values: rods, ovoid rods, or bunches of cones. A mixture of morphologies is found in samples synthesized at the lower pH values or higher pump rates.

These syntheses are a basis for the study of the surface properties of bayerite in relation to their morphology. Each morphology is characterized by particles with different proportions of basal faces, {001}, and lateral faces, such as {111} and {100}.[15] These particles will be used for the measurement of their surface reactivity including acido-basic, sorption, and dissolution properties

Acknowledgment. We thank A. Valette and J. L. Pastol for SEM observations and N. Boisseau for surface area measurements.

CM0310059